Improvement of nuclear semi-empirical mass formula by including shell effect*

Q. Wu (武庆)[1]   W. F. Li (李伟峰)[1]   Z. M. Niu (牛中明)[1†]   H. Z. Liang (梁豪兆)[2,3]   M. Shi (仕敏)[4]

[1]School of Physics and Optoelectronic Engineering, Anhui University, Hefei 230601, China
[2]Department of Physics, Graduate School of Science, The University of Tokyo, Tokyo 113-0033, Japan
[3]Quark Nuclear Science Institute, The University of Tokyo, Tokyo 113-0033, Japan
[4]School of Mathematics and Physics, Anhui Jianzhu University, Hefei 230601, China

Abstract: Shell effect plays an important role in nuclear mass predictions especially for the nuclei around the magic numbers. In this study, a new semi-empirical shell correction terms is constructed to improve the mass description of the Bethe-Weizsäcker (BW) formula. For nuclei with $Z, N \geqslant 8$, the root mean square (rms) deviation of the newly proposed formula with respect to the latest nuclear mass evaluation dataset AME2020 is 0.887 MeV, inducing a 72.23% reduction compared to the rms deviation of 3.194 MeV for the BW formula. The deviations between the theoretical predictions and the experimental data are within 1.5 MeV for 91.90% of the nuclei. In addition, the new mass formula significantly improves the predictions of the binding energies for magic nuclei, the rms deviation of our formula for the binding energy of magic nuclei is only 1.065 MeV, which is a 80.80% reduction compared with that of the BW formula.

Keywords: Nuclear mass, shell correction, semi-empirical formula

I. INTRODUCTION

Nuclear mass is one of the most fundamental physical quantities in nuclear physics [1, 2], which has been widely used to extract nuclear effective interactions [3−6] and various nuclear structure information, such as nuclear pairing correlation [7], shell effect [8, 9], and deformation [10, 11]. From nuclear mass, one can easily calculate the various nucleon separation energies, reaction and decay energies, which determine the positions of the drip lines [12] and are key input to the rapid-neutron capture process simulations (*r*-process). The uncertainty in the nuclear mass has a large influence on the *β*-decay half-lives [13] and the neutron capture rates [14], and then significantly affects the abundance distributions in the *r*-process simulations [15−17]. The *β*-decay half-life calculations with the consideration of first-forbidden transitions also shows the significant impact of mass predictions on half-life calculations and the abundance distributions in the *r*-process simulations. [18]. In conclusion, nuclear mass plays an important role in both nuclear physics and nuclear astrophysics [19−21].

Various theoretical models predict more than 7000 nuclei on the nuclear chart [22−25], but only about 3000 nuclear masses have been experimentally measured [26], and many of the nuclear masses involved in *r*-process simulations remain unmeasured. Therefore, this increases the necessity to develop mass models with reliable extrapolation abilities. At present, various mass models have been developed with rms deviations in the range of 0.3 ~ 3 MeV. There are mainly three kinds of nuclear mass models: macroscopic, microscopic, and macroscopic-microscopic models.

The earliest nuclear mass model was the traditional liquid-drop model, i.e., Bethe-Weizsäcker (BW) semi-empirical formula, which is a macroscopic model that treats the nucleus as a charged liquid drop [27, 28]. Since it does not take into account microscopic shell corrections, there are large deviations between the nuclear mass predictions and the experimental data around magic nuclei, and then the BW formula was developed by including various correction terms [29, 30]. The rms deviation of the improved BW formula reaches about 1.6 MeV. Based on the macroscopic model, the Strutinsky method [31] is

used to extract the shell correction energies, further developing macroscopic-microscopic models. For example, the finite-range droplet model (FRDM) [32, 33] has the rms deviation of about 0.6 MeV with respect to the experimental mass data and is often used as inputs to the *r*-process simulations. In addition, a series of Weizsäcker-Skyrme (WS) models have been developed by taking into account isospin effects [34], mirror nuclei constraints [35], and surface diffuseness effects (WS4) [36]. The WS4 mass model has an rms deviation of about 0.3 MeV. However, it is difficult for macroscopic-microscopic models to ensure self-consistency between macroscopic and microscopic terms. Microscopic models study atomic nuclei at the nucleon level, and can give various nuclear ground-state properties including nuclear mass in a uniform framework [37]. Therefore, they are often believed to have a more reliable extrapolation ability. In a non-relativistic framework, a series of Hartree-Fork-Bogoliubov (HFB) microscopic mass models have been developed with a rms deviation of $0.5 \sim 0.8$ MeV by using Skyrme [38, 39] or Gogny forces [40]. Microscopic mass models in the relativistic framework include Relativistic mean-field (RMF) models [41, 42], Relativistic-Continuum-Hartree-Bogoliubov (RCHB) [22], deformed relativistic Hartree-Bogoliubov theory in continuum (DRHBc) [23, 24, 43]. For these relativistic microscopic mass models, the accuracy with respect to the experimental data now achieves nearly 1 MeV [23, 24, 42]. It should be noted that the DRHBc mass tables were only available for the even-even nuclei [23] and even-Z nuclei [24] nowadays, since the DRHBc calculations are very time consuming due to the inclusion of continuum effects.

In recent years, with the rapid development of artificial intelligence, machine learning (ML) methods have also been widely used to study nuclear properties [44−46], such as *α*-decay half-lives [47, 48], *β*−decay half-lives [49−52], fission yields [53, 54], charge radii [55, 56], nuclear reaction cross sections [57−60]. Currently, ML methods such as Bayesian neural network (BNN) [61−63], kernel ridge regression (KRR) [64, 65], Light Gradient Boosting Machine (LigthGBM) [66], and Gaussian process [67] have been used to study nuclear mass, and the rms deviation of mass models based on these ML methods with respect to the experimental data achieves about 0.1 MeV. Although machine learning models have high prediction accuracy in the known region, the physics basis of ML methods is unclear, which may affect their extrapolation abilities [68]. For example, the radial basis functions (RBF) [69, 70] and KRR methods were found to have reliable extrapolation distances not far from the known region [71]. Recently, the physics-informed machine learning and physics-informed fully connected neural network have been developed to study nuclear mass predictions, which can largely reduce

the discrepancy between theory and experiment by directly learning model binding energy residuals or employing a multi-output training strategy [72, 73].

This study focuses on constructing shell correction terms to improve the prediction ability of the semi-empirical mass formula for magic nuclei. Each term in the semi-empirical mass formula has a clear physical meaning, and it is easy to know the specific contribution of each term to the binding energy. In addition, its high efficiency and low computational cost make it possible to calculate all nuclear masses in a very short time, which is highly useful for systematically studying the uncertainties and sensitivities of the *r*-process. Our mass formula has the rms deviation of 0.887 MeV with respect to the experimental data in AME2020 [26] for nuclei with $Z, N \geqslant 8$, which induces a 72.23% reduction compared to BW formula, and 45.42% lower than the rms deviation of the empirical formula proposed in Ref. [29], and in particular the mass predictions are significantly improved for magic nuclei.

The paper is organized as follows. Sec. II introduces the BW semi-empirical mass formula and construction of the shell correction terms, the results and discussion are presented in Sec. III. Finally, the summary and perspectives are given in Sec. IV.

II. THEORETICAL FRAMEWORK

The traditional BW semi-empirical mass formula takes into account the volume energy, the surface energy, the Coulomb energy, and the symmetry energy. The binding energy *B* for a nucleus with proton numbers *Z* and neutron numbers *N* (mass numbers $A = Z + N$) can be calculated from these four terms:

$$B = \alpha_v A + \alpha_s A^{2/3} + \alpha_c Z^2 A^{-1/3} + \alpha_{sym}(N-Z)^2 A^{-1}, \quad (1)$$

where α_i denotes the free parameters determined by fitting the experimental nuclear masses. In Ref. [29], the exchange Coulomb term $\alpha_{xc} Z^{4/3} A^{-1/3}$, the Wigner term $\alpha_w |N - Z| A^{-1}$, the pairing term $\delta \alpha_p A^{-1/2}$, the surface symmetry term $\alpha_{st}(N-Z)^2 A^{-4/3}$, the curvature term $\alpha_r A^{1/3}$, and the shell correction terms $\alpha_m P + \beta_m P^2$ based on the BW formula are added. In this paper, this model is denoted as the BWK mass formula. In the above expressions, δ and P are given by.

$$\delta = \frac{(-1)^Z + (-1)^N}{2}, \quad (2)$$

$$P = \frac{\nu_p \nu_n}{\nu_p + \nu_n}, \quad (3)$$

where ν_p and ν_n are the number of valence nucleons, i.e.,

the differences between the nucleon numbers Z and N and the nearest magic number (the proton and neutron magic numbers are taken to be 2, 8, 20, 28, 50, 82, 126 and 2, 8, 20, 28, 50, 82, 126, 184 as in Ref. [29]). The new formula obtained by removing the shell correction terms $\alpha_m P + \beta_m P^2$ from BWK formula is denoted as BWK* formula.

In Fig. 1, we investigate the effect of the shell correction terms $\alpha_m P + \beta_m P^2$ in the BWK formula on the predictions of binding energies. In general, the term gives a large improvement in the predictions of binding energies, causing a reduction of the rms deviation by about 0.8 MeV, especially, it improves the predictions of the binding energies of some deformed nuclei, such as those in the regions $32 \lesssim Z \lesssim 41$ and $34 \lesssim N \lesssim 45$, $34 \lesssim Z \lesssim 47$, and $57 \lesssim N \lesssim 73$. In addition, BWK formula also improves the prediction ability of the binding energies for some magic nuclei with $N = 28, 50$. However, the predictions of the BWK formula have been worse for nuclei with $Z \approx 50, 82$, overestimating the experimental binding energies to above 4 MeV, while the predictions for some doubly magic nuclei are underestimated by more than 4 MeV. Moreover, the shell correction energies between semi-magic and doubly magic nuclei should be different, while the shell correction terms $\alpha_m P + \beta_m P^2$ are always 0 for both semi-magic and doubly magic nuclei, so it is ne-

cessary to construct a new shell correction term that reflects the difference in shell correction energies between semi-magic and doubly magic nuclei.

To construct appropriate shell correction terms for magic nuclei, we study the differences between the experimental binding energies of around magic nuclei and the BWK predictions with respect to the number of valence nucleons, which are shown in Fig. 2. The binding energy residuals of the BWK formula are found to have an approximate linear relationship with the number of valence nucleons when the mass number $A \geqslant 56$. Therefore, the linear term of valence nucleons $c_m(\nu_n + \nu_p)$ is used to describe the residuals of the semi-magic nuclear binding energy. The new formula is denoted as F1, and the form is as follows:

$$
\begin{aligned}
B = {} & \alpha_v A + \alpha_s A^{2/3} + \alpha_c Z^2 A^{-1/3} + \alpha_{sym}(N-Z)^2 A^{-1} \\
& + \delta \alpha_p A^{-1/2} + \alpha_{xc} Z^{4/3} A^{-1/3} \\
& + \alpha_w |N-Z| A^{-1} + \alpha_{st}(N-Z)^2 A^{-4/3} \\
& + \alpha_r A^{1/3} + \alpha_m P + \beta_m P^2 + c_m(\nu_n + \nu_p),
\end{aligned}
\tag{4}
$$

It is found that the linear term $c_m(\nu_n + \nu_p)$ has very little effect on the prediction of the binding energy for nuclei with $A < 56$. In order to make the formula more universal, the linear term is used to improve the description of the binding energy for all nuclei with $Z, N \geqslant 8$.

It can be seen from Fig. 1(b) that the residuals between the experimental binding energies and the predictions calculated with the BWK formula are largest near the doubly magic nuclei and decrease away from them. The exponential term $e_{m1} e^{e_{m2}(\nu_p^2 + \nu_n^2)}$ is introduced to describe such residuals for doubly magic nuclei similar to Refs. [74, 75], where e_{m1} is expected to be positive and is the shell correction energies of the doubly magic nuclei,
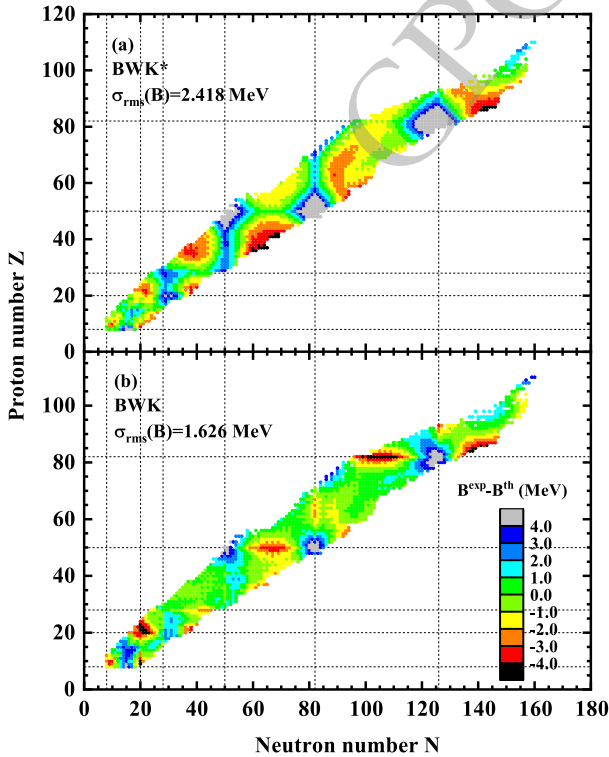

Fig. 1. (color online) The differences between the experimental binding energies and the predictions calculated with the BWK* and BWK formulas, respectively. The dashed lines denote the traditional magic numbers.
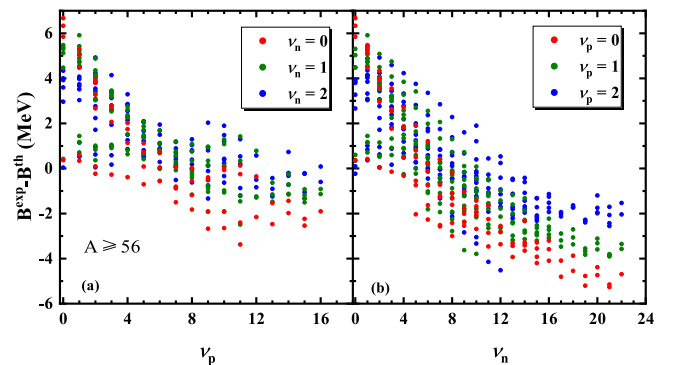

Fig. 2. (color online) Binding energy differences between the experimental data and the predictions calculated with the BWK formula for nuclei with $A \geqslant 56$ as a function of the $\nu_p(a)$ and $\nu_n(b)$ when number of valence nucleons are 0 (red solid circle), 1 (green solid circle), and 2 (blue solid circle), respectively.

and e_{m2} is expected to be negative in order that the term gradually decays to 0 when moving away from the magic number. The new formula with exponential term $e_{m1}e^{e_{m2}(\nu_p^2+\nu_n^2)}$ are denoted as F2*. The isospin dependence is further introduced in F2* formula as in Ref. [36], the new formula is denoted as F2. The specific expressions of F2* and F2 mass formulas are.

$$
\begin{aligned}
B = {}& \alpha_v A + \alpha_s A^{2/3} + \alpha_c Z^2 A^{-1/3} + \alpha_{sym}(N-Z)^2 A^{-1} \\
& + \delta \alpha_p A^{-1/2} + \alpha_{xc} Z^{4/3} A^{-1/3} \\
& + \alpha_w |N-Z| A^{-1} + \alpha_{st}(N-Z)^2 A^{-4/3} \\
& + \alpha_r A^{1/3} + \alpha_m P + \beta_m P^2 + c_m(\nu_n + \nu_p) \\
& + e_{m1} e^{e_{m2}(\nu_p^2+\nu_n^2)},
\end{aligned}
\tag{5}
$$

$$
\begin{aligned}
B = {}& \alpha_v A + \alpha_s A^{2/3} + \alpha_c Z^2 A^{-1/3} + \alpha_{sym\_1} I^2 A f_s \\
& + \delta_{np} \alpha_p A^{-1/3} + \alpha_{xc} Z^{4/3} A^{-1/3} + \alpha_r A^{1/3} \\
& + \alpha_m P + \beta_m P^2 + c_m(\nu_n + \nu_p) \\
& + e_{m1} e^{e_{m2}(\nu_p^2+\nu_n^2)},
\end{aligned}
\tag{6}
$$

where α_{sym_1}, I, f_s, and δ_{np} are defined as.

$$
\alpha_{sym\_1} = c_{sym}\left(1 - \frac{k}{A^{1/3}} + \xi \frac{2-|I|}{2+|I|A}\right),
\tag{7}
$$

$$
I = \frac{N-Z}{A},
\tag{8}
$$

$$
f_s = 1 + \kappa_s\left(\left(I - \frac{0.4A}{A+200}\right)^2 - I^4\right) A^{1/3},
\tag{9}
$$

$$
\delta_{np} = \begin{cases}
(2-|I|-I^2)17/16, & N \text{ and } Z \text{ even} \\
|I|-I^2, & N \text{ and } Z \text{ odd} \\
1-|I|, & N \text{ even}, Z \text{ odd, and } N > Z \\
1-|I|, & N \text{ odd}, Z \text{ even, and } N < Z \\
1, & N \text{ even}, Z \text{ odd, and } N < Z \\
1, & N \text{ odd}, Z \text{ even, and } N > Z.
\end{cases}
\tag{10}
$$

It is worth noting that symmetry energy term with isospin dependence in the Eq. (6) can be expanded by three terms, the symmetry energy term, the surface symmetry term, and the Wigner term. From Fig. 1(b), it is seen that the residuals of doubly magic nuclei are negative in the light-mass region, positive in the heavy-mass region, and near zero in the medium-mass region. In addition, we have tried many improvement methods and found that the

corresponding binding energy residuals always have same phenomenon. This means that the residuals of the binding energies are different for the magic nuclei in different regions. In order to describe the differences between the magic nuclei of different regions, a δ_{shell} in the coefficient of the exponential term is introduced, and the new formula obtained is named BWN, whose expression is.

$$
\begin{aligned}
B = {}& \alpha_v A + \alpha_s A^{2/3} + \alpha_c Z^2 A^{-1/3} + \alpha_{sym\_1} I^2 A f_s \\
& + \delta_{np} \alpha_p A^{-1/3} + \alpha_{xc} Z^{4/3} A^{-1/3} + \alpha_r A^{1/3} \\
& + \alpha_m P + \beta_m P^2 + c_m(\nu_n + \nu_p) \\
& + e_{m1} \delta_{shell} e^{e_{m2}(\nu_p^2+\nu_n^2)},
\end{aligned}
\tag{11}
$$

where

$$
\delta_{shell} = \begin{cases}
-1, & Z, N \in [8,24], \\
0, & Z \in [8,24] \ \& \ N \in (24,66), \\
0, & Z \in (24,39] \ \& \ N \in [8,66], \\
1, & \text{elsewhere}.
\end{cases}
\tag{12}
$$

The parameters and corresponding uncertainties of semi-empirical formulas, i.e., BW, BWK*, BWK, F1, F2*, F2, and BWN, are obtained by performing a least squares fit on the experimental data for nuclei with $Z, N \geqslant 8$ in AME2020 [26], which are shown in Tables 1 and 2. The mass tables for the F1, F2*, F2, and BWN formulas are available as the Supplemental Material of this paper The accuracy of the semi-empirical formula is evaluated by the rms deviation, defined by:

$$
\sigma_{rms}(B) = \sqrt{\sum_{i=1}^{n}(B_i^{exp} - B_i^{th})^2/n},
\tag{13}
$$

where B_i^{exp} and B_i^{th} are the experimental binding energies and the theoretical predictions, respectively. n is the number of experimental data for the nuclei with $Z, N \geqslant 8$.

III. RESULTS AND DISCUSSION

The rms deviations of the binding energies and single-neutron (proton) separation energies calculated by each semi-empirical formula are shown in Tables 1 and 2. From Tables 1 and 2, it is seen that the rms deviation of the newly proposed BWN formula is 0.887 MeV, which is 72.23%, 45.42% less than the BW and BWK formulas, respectively. Since the rms deviations of F2* and F2 formulas are similar, isospin dependence in the symmetry energy and pairing energy terms in F2 formula does not

Table 1.   Parameters with uncertainties and σ_{rms} of the BW, BWK, BWK*, and F1 mass formulas.

	BW	BWK	BWK*	F1
α_v(MeV)	15.5255 ± 0.0242	16.4920 ± 0.0659	16.1707 ± 0.0954	16.3845 ± 0.0507
α_s(MeV)	-16.8949 ± 0.0753	-25.5618 ± 0.4630	-23.5820 ± 0.6695	-24.7173 ± 0.3566
α_c(MeV)	-0.7022 ± 0.0017	-0.7614 ± 0.0031	-0.7408 ± 0.0044	-0.7611 ± 0.0024
$\alpha_{sym}(c_{sym})$(MeV)	-22.9874 ± 0.0603	-32.5777 ± 0.3042	-31.7110 ± 0.4440	-31.8596 ± 0.2346
α_p(MeV)	–	11.0409 ± 0.4608	11.9953 ± 0.6844	11.1655 ± 0.3543
α_{xc}(MeV)	–	1.6997 ± 0.0743	1.4587 ± 0.1077	1.8009 ± 0.0572
α_w(MeV)	–	-61.7229 ± 2.8712	-57.7605 ± 4.2667	-44.4585 ± 2.2473
α_{st}(MeV)	–	61.1172 ± 1.5853	57.5972 ± 2.3234	55.2362 ± 1.2273
α_r(MeV)	–	13.3315 ± 0.7883	10.0163 ± 1.1482	11.2350 ± 0.6083
α_m(MeV)	–	-2.0293 ± 0.0419	–	-1.1379 ± 0.0389
β_m(MeV)	–	0.1595 ± 0.0045	–	0.1979 ± 0.0036
c_m(MeV)	–	–	–	-0.3665 ± 0.0089
e_{m1}(MeV)	–	–	–	–
e_{m2}	–	–	–	–
k	–	–	–	–
ξ	–	–	–	–
κ_s	–	–	–	–
$\sigma_{\mathrm{rms}}(B)$(MeV)	3.194	1.625	2.418	1.250
$\sigma_{\mathrm{rms}}(S_n)$(MeV)	1.335	0.585	0.639	0.509
$\sigma_{\mathrm{rms}}(S_p)$(MeV)	1.542	0.614	0.600	0.507

Table 2.   Parameters with uncertainties and σ_{rms} of the F2*, F2, and BWN mass formulas.

	F2*	F2	BWN
α_v(MeV)	16.1287 ± 0.0482	15.9108 ± 0.0474	16.7043 ± 0.0398
α_s(MeV)	-21.9924 ± 0.3502	-19.5107 ± 0.3376	-26.3000 ± 0.2824
α_c(MeV)	-0.7542 ± 0.0023	-0.7404 ± 0.0025	-0.7615 ± 0.0020
$\alpha_{sym}(c_{sym})$(MeV)	-31.3853 ± 0.2205	-33.1442 ± 0.3409	-35.3636 ± 0.2648
α_p(MeV)	11.4215 ± 0.3248	6.0387 ± 0.1634	5.9751 ± 0.1303
α_{xc}(MeV)	1.6434 ± 0.0534	1.2311 ± 0.0592	1.4405 ± 0.0473
α_w(MeV)	-41.1184 ± 2.0908	–	–
α_{st}(MeV)	52.1968 ± 1.1617	–	–
α_r(MeV)	2.9261 ± 0.6888	-2.1600 ± 0.6452	14.1287 ± 0.4749
α_m(MeV)	-1.0094 ± 0.0379	-1.0369 ± 0.0369	-1.0877 ± 0.0277
β_m(MeV)	0.1008 ± 0.0058	0.1052 ± 0.0057	0.1615 ± 0.0028
c_m(MeV)	0.0399 ± 0.0264	0.0318 ± 0.0257	-0.2343 ± 0.0076
e_{m1}(MeV)	7.6167 ± 0.4509	7.3839 ± 0.4407	5.4713 ± 0.1229
e_{m2}	-0.0104 ± 0.0004	-0.0103 ± 0.0004	-0.0444 ± 0.0020
k	–	1.9017 ± 0.0417	2.0829 ± 0.0288
ξ	–	1.9050 ± 0.0434	1.2216 ± 0.0313
κ_s	–	0.2417 ± 0.0405	0.2491 ± 0.0314
$\sigma_{\mathrm{rms}}(B)$(MeV)	1.144	1.111	0.887
$\sigma_{\mathrm{rms}}(S_n)$(MeV)	0.483	0.417	0.381
$\sigma_{\mathrm{rms}}(S_p)$(MeV)	0.481	0.450	0.394

improve the accuracy in the known region, although their differences may become large in the unknown region. Furthermore, compared with F2 formula, the introduction of δ_{shell} in BWN formula can reduce the rms deviation by approximately 0.2 MeV, which indicates the importance of employing different shell corrections in different mass regions. In addition, BWN formula not only improves the description of the nuclear mass, but also significantly improves the prediction accuracies of the single-neutron (proton) separation energy. Among these mass formulas, the BWN mass formula is the only one whose rms deviations with respect to both the experimental single-neutron separation energies and the experimental single-proton separation energies are below 0.4 MeV. As can be seen in Fig. 2, the coefficient of the linear term for the number of valence nuclei should be negative. However, it is noted that the parameters c_m in the F2* and F2 formulas are positive, which are opposite to the sign we expected. This indicates that the exponential term with a constant coefficient does not accurately describe the shell correction energies of magic nuclei. The constant coefficient exponential term may unreasonably provide a part of shell correction energies for semi-magic nuclei in some degree, which induces the sign of the parameter of the linear term does not match what we expected. In contrast, the BWN formula has more reasonable parameters by taking into account the difference in shell correction energies of magic nuclei with different masses. In addition, it is worth mentioning that compared with the BW formula, the introduction of the surface symmetry term and the exchange Coulomb term leads to the surface energy and Coulomb energy coefficients in the BWN formula to be slightly different from the corresponding coefficients in BW formula.

The rms deviation can only roughly reflect the accuracy of a semi-empirical mass formula. To show more details, the differences between the experimental binding energies and the predictions calculated by the F1, F2* and F2 formulas are shown in Fig. 3 Compared with Fig. 1(b), it can be found from Fig. 3(a) that the introduction

of the linear terms $c_m(v_n + v_p)$ improves the prediction ability of the formula for nuclei with proton numbers around 50, 82 and reduces the rms deviation by about 0.4 MeV. From Fig. 3(a) and (b), it can be seen that the exponential term with a constant coefficient provides a slight improvement for some superheavy nuclei, such as nuclei with $Z \geqslant 82$ and $N \geqslant 126$, but does not significantly improve the prediction accuracy of binding energies for doubly magic nuclei. Furthermore, comparing Fig. 3(b) and (c), we find that the effect of the isospin dependence of the symmetric energy and the pairing energy term on mass description is small in the known mass region, with the rms deviation decreasing by about 0.03 MeV.

The mass description of the newly improved BWN formula is compared with the BW formula as shown in Fig. 4, it can be seen that the binding energy predictions of the BW formula have large deviations from the experimental binding energies for magic nuclei and most deformed nuclei. Around the doubly magic nuclei, the predictions of the BW formula are always underestimated by more than 4 MeV compared to the experimental binding energies, while they are overestimated by more than 4 MeV in the deformation regions, such as $31 \lesssim Z \lesssim 39$ and $35 \lesssim N \lesssim 47$, $38 \lesssim Z \lesssim 47$ and $55 \lesssim N \lesssim 69$, $Z \gtrsim 82$ and $N \gtrsim 126$. In addition, the binding energy residuals calculated by BW formula Eq. (1) show odd-even staggering structures due to the lack of odd-even pairing correction, i.e. smaller and larger differences appear alternately. Compared to the BW formula, it can be seen from Fig. 4(b) that the BWN formula significantly improves the description of nuclear binding energies for nuclei near the magic numbers and the deformed nuclei. Based on the F2 formula, the BWN formula further takes into account the differences between doubly magic nuclei in different regions by introducing δ_{shell}, its mass description is significantly improved in the region around the doubly magic nuclei, and the prediction accuracy of nuclear binding energies in the $8 < Z < 20$, $8 < N < 20$ region is also improved. The rms deviations of the predictions of the BWN formula with respect to the experimental binding
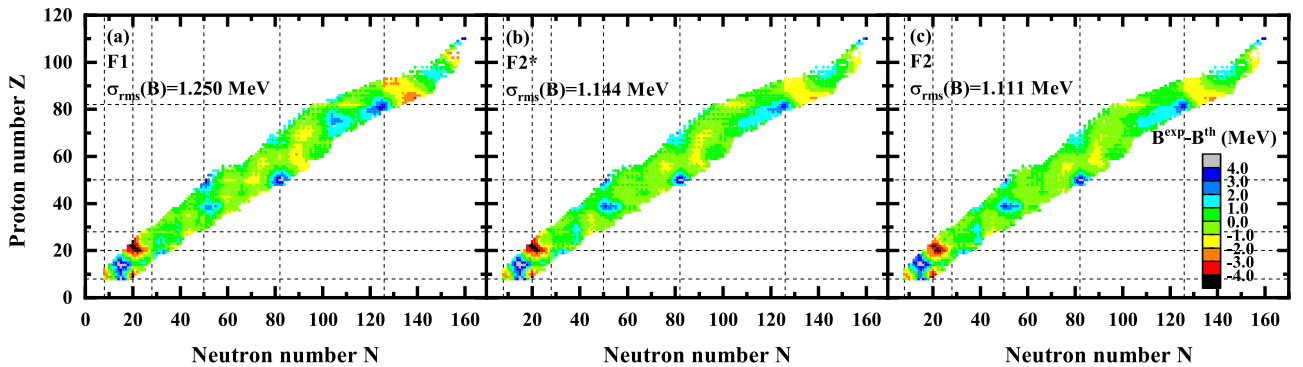

Fig. 3. (color online) The differences between the experimental binding energies and the predictions calculated with the F1, F2*, and F2 formulas. The dashed lines denote the traditional magic numbers.
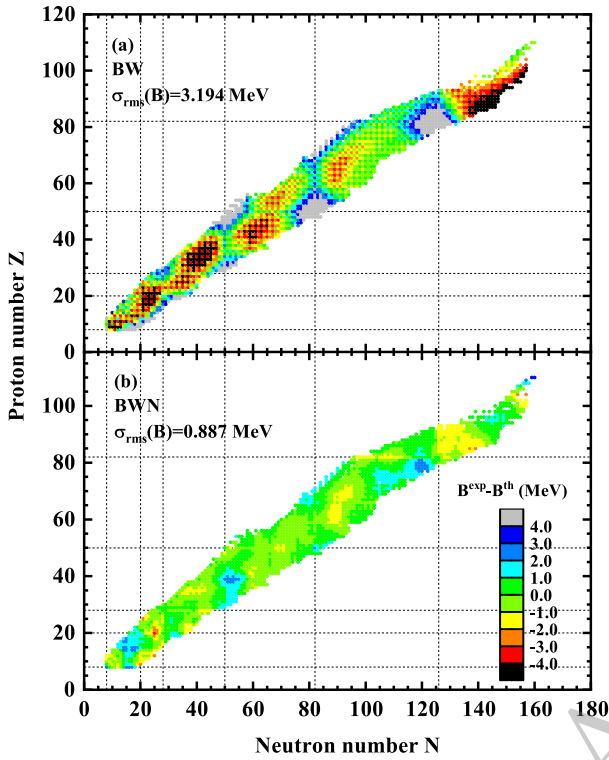
Fig. 4. (color online) The differences between the experimental binding energies and the predictions calculated with the BW and BWN formulas. The dashed lines denote the traditional magic numbers.

Fig. 5. (color online) The differences between the experimental nuclear binding energies and the predictions calculated with the BW (grey squares), BWK (blue triangles), and BWN (red circles) formulas versus proton and neutron numbers.

energies are 0.887, 0.838, and 1.065 MeV for the three data sets: Z, $N \geqslant 8, A \geqslant 60$, and the magic nuclei, respectively, which is a reduction of 72.23%, 73.35% and 80.08%, respectively, compared with the BW formula.

In Fig. 5, the differences between the experimental binding energies and the predictions of the BW, BWK, and BWN mass formulas as a function of proton number and neutron number are shown. The differences between the experimental binding energies and the predictions of the BW mass formula are very large in the light nuclei region and in regions with proton numbers $Z = 50, 82$ or neutron numbers $N = 50, 82, 126$, and even reach more than 15 MeV. In addition to the region around traditional magic numbers, the large differences between experimental binding energies and the BW predictions are also found for some nuclei, such as those around $Z = 34, 90$ or $N = 40, 145$. By including other correction terms, the BWK formula reduces the binding energy residuals for most nuclei, but its predictions are not more accurate than BW for part nuclei, e.g., the nuclei with $100 \lesssim N \lesssim 120$. Based on the BWK formula, BWN formula is obtained by including new shell correction terms, the descriptions of the nuclear mass is further improved for magic nuclei. The rms deviations of the BW, BWK formulas with respect to magic nuclei are 5.346 MeV and 2.729 MeV, respectively, while the corresponding rms deviation of the
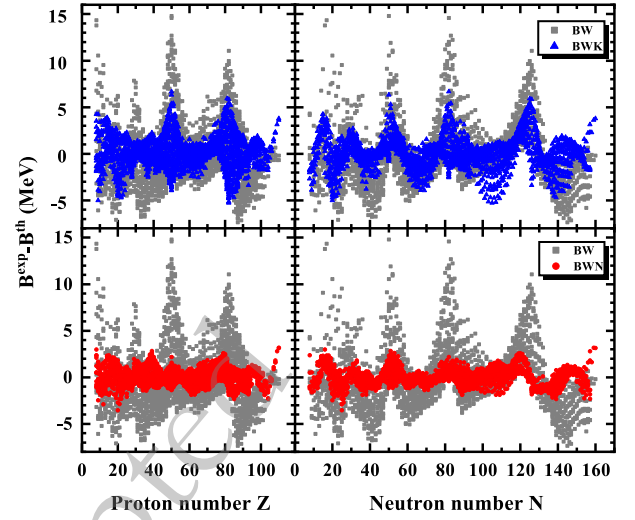
BWN formula is only 1.065 MeV, which is reduced by 80.80% and 60.97% compared to that of the BW and BWK formulas, respectively. In addition, the differences between the experimental binding energies and the BWN predictions are almost always within 1.5 MeV. The percentage of nuclei for which the predictions of BW, BWK, and BWN deviate from the experimental data within 1.5 MeV is 41.88%, 70.21%, and 91.90%, respectively.

The single-neutron separation energies S_n of the BW, BWK, and BWN mass formulas are shown in Fig. 6, taking the Ca, Ni, Sn, and Pb isotopes as examples. There is remarkable odd-even staggering for the S_n in each isotopes. The S_n variation is smooth for the BW formula in Eq. (1) due to the ignorance of the pairing term, whereas the BWK and BWN formulas well reproduce the odd-even staggering. The experimental S_n shows a sudden decrease after the neutron magic numbers, e.g. S_n decreases sharply from 7.353 MeV of ^{132}Sn to 2.399 MeV of ^{133}Sn. The BWN formula better reproduces the S_n of nuclei with neutron magic numbers in the Sn and Pb isotopic chains than the BWK formula. Similarly, the single-proton separation energies S_p predicted by the BW, BWK, and BWN formulas for $N = 20, 28, 50, 82, 126$ isotones are shown in Fig. 7. It can be seen from Fig. 7 that both BWK and BWN formula reproduce the experimental S_p well, but the BWN formula better reproduces the experimental S_p near the proton magic numbers than the BWK formula. Therefore, the BWN formula shows better agreement with the experimental masses and separation energies than the BW and BWK formulas, particularly for nuclei around magic numbers.
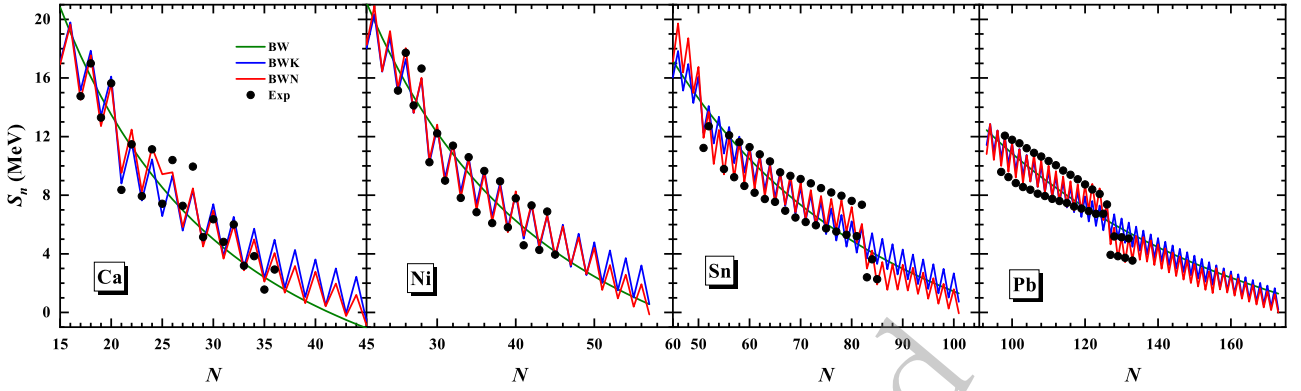
Fig. 6. (color online) Single-neutron separation energies of Ca, Ni, Sn, and Pb isotopes predicted by BW, BWK, and BWN. The experimental data from AME2020 are denoted by filled circle.
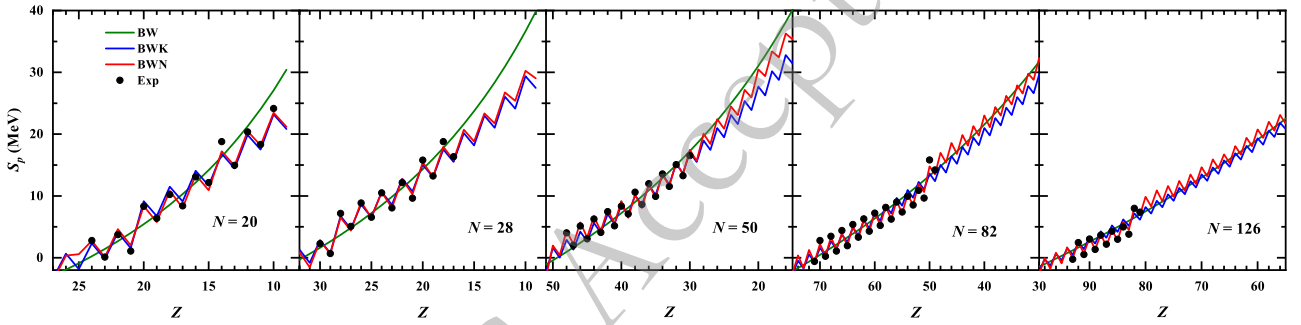

Fig. 7. (color online) Same to Fig. 6, but for single-proton separation energies S_p of $N = 20, 28, 50, 82, 126$ isotones.

IV. SUMMARY AND PERSPECTIVES

In summary, a semi-empirical mass formula based on liquid-drop model is improved by including new shell correction terms. The shell correction terms in the mass formula contain three components: the quadratic polynomial of P, the linear, and the exponential term of valence nucleons. The quadratic polynomial terms of P improve the predictions of binding energy for most deformed nuclei and part magic nuclei. The linear term for the number of valence nucleons is used to improve the prediction ability of the mass formula for semi-magic nuclei, especially the nuclei with proton numbers near 50, 82 and reduces the rms deviation by approximately 0.4 MeV. The introduction of an exponential term with a constant coefficient did not obviously improve the prediction ability of the mass formula for doubly magic nuclei, but the binding energy residuals were significantly reduced for doubly nuclei by taking into account the differences between the different doubly magic nuclei, and the exponential term reduces the rms deviation by about 0.2 MeV. Compared with the BW and BWK mass formula, the rms deviation of our mass formula with respect to experi-

mental data for the nuclei with $Z, N \geqslant 8$ is reduced by 72.23% and 45.42%, respectively, and falls to 0.887 MeV. The rms deviation of the our formula with respect to magic nuclei is only 1.065 MeV, which is reduced by 80.80% and 60.97% compared to those of the BW and BWK formulas, respectively. In addition, nuclei with experimental binding energies that deviate from the predictions of BW, BWK, and our mass formula within 1.5 MeV account for 41.88%, 70.21% and 91.90% of the total number of nuclei, respectively. Besides the significant improvement in the description of nuclear mass, our mass formula also improves the predictions of mass differences, such as the single-neutron (proton) separation energy. In conclusion, our mass formula significantly improves the description of nuclear binding energies, especially for magic nuclei. In the future, we will further consider the effect of deformed effects on the binding energy. In addition, since the semi-empirical formula enables large-scale calculations of nuclear masses in a short time, it is well suited for studies of the sensitivity of *r*-process abundances to nuclear masses, which could deepen our understanding of the origin of heavy elements.

References

[1]   D. Lunney, J. M. Pearson, and C. Thibault, Rev. Mod. Phys. **75**, 1021 (2003)

[2]   M. Bender, P. H. Heenen, and P. G. Reinhard, Rev. Mod. Phys. **75**, 121 (2003)

[3] P. W. Zhao, Z. P. Li, J. M. Yao, and J. Meng, Phys. Rev. C **82**, 054319 (2010)

[4] S. Goriely, N. Chamel, and J. M. Pearson, Phys. Rev. C **88**, 061302 (2013)

[5] Q. Zhao, Z. X. Ren, P. W. Zhao, and J. Meng, Phys. Rev. C **106**, 034315 (2022)

[6] Z. X. Liu, Y. H. Lam, N. Lu, and P. Ring, Phys. Lett. B **842**, 137946 (2023)

[7] W. Satula, J. Dobaczewski, and W. Nazarewicz, Phys. Rev. Lett. **81**, 3599 (1998)

[8] M. E. Ramirez, D. Ackermann, K. Blaum et al., Science **337**, 1207 (2012)

[9] F. Wienholtz, D. Beck, K. Blaum et al., Nature **498**, 346 (2013)

[10] U. Hager, T. Eronen et al., Phys. Rev. Lett. **96**, 042504 (2006)

[11] A. de Roubin, D. Atanasov et al., Phys. Rev. C **96**, 014310 (2017)

[12] E. Jochen, B. Noah, K. Markus et al., Nuture **486**, 509 (2012)

[13] M. Shi, J. Y. Fang, and Z. M. Niu, Chin. Phys. C **45**, 044103 (2021)

[14] C. Ma, Z. Li, Z. M. Niu, and H. Z. Liang, Phys. Rev. C **100**, 024330 (2019)

[15] M. R. Mumpower, R. Surman, D.-L. Fang, M. Beard, P. Möller, T. Kawano, and A. Aprahamian, Phys. Rev. C **92**, 035807 (2015)

[16] X. F. Jiang, X. H. Wu, and P. W. Zhao, Astrophys. J. **915**, 29 (2021)

[17] Y. W. Hao, Y. F. Niu, and Z. M. Niu, Phys. Lett. B **844**, 138092 (2023)

[18] T. Marketin, L. Huther, and G. Martínez-Pinedo, Phys. Rev. C **93**, 025805 (2016)

[19] H. A. Bethe, Phys. Rev. **55**, 434 (1939)

[20] M. R. Mumpower, R. Surman, G. C. McLaughlin, and A. Aprahamian, Prog. Part. Nucl. Phys. **86**, 86 (2016)

[21] J. J. Cowan, C. Sneden, J. E. Lawler, A. Aprahamian, M. Wiescher, K. Langanke, G. Martínez-Pinedo, F.-K. Thielemann, Rev. Mod. Phys. **93**, 015002 (2021)

[22] X. W. Xia, Y. Lim, P. W. Zhao, H. Z. Liang et al., Atomic Data Nucl. Data Tables **121-122**, 1 (2018)

[23] K. Y. Zhang, M. K. Cheoun, Y. B. Choi, P. S. Chong, J. M. Dong et al., Atomic Data Nucl. Data Tables **144**, 101488 (2022)

[24] P. Guo, X. J. Xiao, K. M. Chen, Z. H. Chen, M. K. Cheoun, Y. B. Choi et al., Atomic Data Nucl. Data Tables **158**, 101661 (2024)

[25] Z. X. Liu, Y. H. Lam, N. Lu, and P. Ring, Atomic Data Nucl. Data Tables **156**, 101635 (2024)

[26] M. Wang, W. J. Huang, F. G. Kondev et al., Chin. Phys. C **45**, 030003 (2021)

[27] C. F. Von Weizsäcker, Z. Phys. **96**, 431 (1935)

[28] H. A. Bethe and R. F. Bacher, Rev. Mod. Phys. **8**, 82 (1936)

[29] M. W. Kirson, Nucl. Phys. A **798**, 29 (2008)

[30] X. Y. Xu, L. Deng, A. X. Chen, H. Yang, H. Jalili, and H. K. Wang, Nucl. Sci. Tech. **35**, 91 (2024)

[31] V. M. Strutinsky, Nucl. Phys. A **95**, 420 (1967)

[32] P. Möller, J. R. Nix, W. D. Myers et al., Atomic Data Nucl. Data Tables **59**, 185 (1995)

[33] P. Möller, W. D. Myers, H. Sagawa, and S. Yoshida, Phys. Rev. Lett. **108**, 052501 (2012)

[34] N. Wang, M. Liu, and X. Z. Wu, Phys. Rev. C **81**, 044322 (2010)

[35] N. Wang, Z. Y. Liang, M. Liu et al., Phys. Rev. C **82**, 044304 (2010)

[36] N. Wang, M. Liu, X. Z. Wu, and J. Meng, Phys. Lett. B **734**, 215 (2014)

[37] J. Meng, H. Toki, S. G. Zhou, S. Q. Zhang, W. H. Long, and L. S. Geng, Prog. Part. Nucl. Phys. **57**, 470 (2006)

[38] S. Goriely, N. Chamel, and J. M. Pearson, Phys. Rev. Lett. **102**, 152503 (2009)

[39] S. Goriely, N. Chamel, and J. M. Pearson, Phys. Rev. C **93**, 034337 (2016)

[40] S. Goriely, S. Hilaire, M. Girod et al., Phys. Rev. Lett. **102**, 242501 (2009)

[41] L. S. Geng, H. Toki, and J. Meng, Prog. Theor. Phys. **113**, 785 (2005)

[42] D. Peña-Arteaga, S. Goriely, and N. Chamel, Eur. Phys. J. A **52**, 320 (2016)

[43] S. G. Zhou, J. Meng, P. Ring, and E. G. Zhao, Phys. Rev. C **82**, 011301(R) (2010)

[44] A. Boehnlein, M. Diefenthaler, N. Sato, M. Schram, V. Ziegler, C. Fanelli, M. Hjorth-Jensen, T. Horn et al., Rev. Mod. Phys. **94**, 031003 (2022)

[45] W. B. He, Q. F. Li, Y. G. Ma, Z. M. Niu, J. C. Pei, and Y. X. Zhang, Sci. China Phys. Mech. Astron. **66**, 282001 (2023)

[46] W. B. He, Y. G. Ma, L. G. Pang, H. C. Song, and K. Zhou, Nucl. Sci. Tech. **34**, 88 (2023)

[47] N. N. Ma, X. J. Bao, and H. F. Zhang, Chin. Phys. C **45**, 024105 (2021)

[48] Z. Y. Yuan, D. Bai, Z. Z. Ren, and Z. Wang, Chin. Phys. C **46**, 024101 (2022)

[49] N. J. Costiris, E. Mavrommatis, K. A. Gernoth, and J. W. Clark, Phys. Rev. C **80**, 044332 (2009)

[50] Z. M. Niu, H. Z. Liang, B. H. Sun, W. H. Long, and Y. F. Niu, Phys. Rev. C **99**, 064307 (2019)

[51] W. F. Li, X. Y. Zhang, Y. F. Niu, and Z. M. Niu, J. Phys. G: Nucl. Part. Phys. **51**, 015103 (2024)

[52] P. Li, Z. M. Niu, and Y. F. Niu, Nucl. Sci. Tech. **36**, 50 (2025)

[53] Z. A. Wang, J. C. Pei, Y. Liu, and Y. Qiang, Phys. Rev. Lett. **123**, 122501 (2019)

[54] A. E. Lovell, A. T. Mohan, and P. Talou, J. Phys. G: Nucl. Part. Phys. **47**, 114001 (2020)

[55] S. Akkoyun, T. Bayram, S. O. Kara, and A. Sinan, J. Phys. G: Nucl. Part. Phys. **40**, 055106 (2013)

[56] Y. F. Ma, C. Su, J. Liu, Z. Z. Ren, C. Xu, and Y. H. Gao, Phys. Rev. C **101**, 014304 (2020)

[57] T. X. Huang, X. H. Wu, and P. W. Zhao, Commun. Theor. Phys. **74**, 095302 (2022)

[58] Y. Y. Li, F. Zhang, J. Su, Nucl. Sci. Tech. **33**, 135 (2022)

[59] W. F. Li, L. L. Liu, Z. M. Niu, Y. F. Niu, and X. L. Huang, Phys. Rev. C **109**, 044616 (2024)

[60] Q. K. Sun, Y. Zhang, Z. R. Hao, H. W. Wang, G. T. Fan et al., Nucl. Sci. Tech. **36**, 52 (2025)

[61] R. Utama, J. Piekarewicz, H. B. Prosper, Phys. Rev. C **93**, 014311 (2016)

[62] Z. M. Niu and H. Z. Liang, Phys. Lett. B **778**, 48 (2018)

[63] Z. M. Niu and H. Z. Liang, Phys. Rev. C **106**, L021303 (2022)

[64] X. H. Wu, L. H. Guo, and P. W. Zhao, Phys. Lett. B **819**, 136387 (2021)

[65] X. H. Wu, Y. Y. Lu, and P. W. Zhao, Phys. Lett. B **834**, 137394 (2022)

[66] Z. P. Gao, Y. J. Wang, H. L. Lv, Q. F. Li, C. W. Shen, and

L. Liu, Nucl. Sci. Tech. **32**, 109 (2021)

[67] Z. Y. Yuan, D. Bai, Z. Wang, and Z. Z. Ren, Nucl. Sci. Tech. **35**, 105 (2024)

[68] Z. M. Niu, J. Y. Fang, and Y. F. Niu, Phys. Rev. C **100**, 054311 (2019)

[69] Z. M. Niu, Z. L. Zhu, Y. F. Niu, B. H. Sun, T. H. Heng, and J. Y. Guo, Phys. Rev. C **88**, 024325 (2013)

[70] Z. M. Niu, B. H. Sun, H. Z. Liang *et al.*, Phys. Rev. C **94**, 054315 (2016)

[71] X. H. Wu and P. W. Zhao, Phys. Rev. C **101**, 051301 (2020)

[72] I. Bentley, J. Tedder, M. Gebran, and A. Paul, Phys. Rev. C **111**, 034305 (2025)

[73] Y. M. Huang, J. H. Chen, J. Y. Jia, L.-M. Liu, Y.-G. Ma, and C. J. Zhang, Phys. Rev. C **111**, 034329 (2025)

[74] X. P. Zhang, Z. Z. Ren, Q. J. Zhi, and Q. Zheng, J. Phys. G: Nucl. Part. Phys. **34**, 2611 (2007)

[75] Y. Zhou, Z. H. Li, Y. B. Wang, Y. S. Chen, B. Guo, J. Su *et al.*, Sci. China-Phys. Mech. Astron. **60**, 082012 (2017)